International Journal on Interactive Design and Manufacturing (IJIDeM)
https://doi.org/10.1007/s12008-024-01777-3

ORIGINAL ARTICLE

Multi-objective optimization of machining parameters for Si_3N_4–BN reinforced magnesium composite in wire electrical discharge machining

S. Sudhagar[1] · P. M. Gopal[2] · M. Maniyarasan[3] · S. Suresh[4] · V. Kavimani[2]

Received: 30 November 2023 / Accepted: 6 February 2024

Abstract
The present research examines the impact of Si_3N_4–BN hybrid reinforcement on the machinability of a magnesium hybrid composite in wire electrical discharge machine (WEDM). The composite is fabricated through inert gas assisted stir casting route with silicon nitride and boron nitride as reinforcement with varying weight percentages of 0%, 5%, and 10%. Subsequently, the fabricated composites were machined through WEDM according to Taguchi 27 orthogonal array with varying pulse on time (PON), pulse off time (POFF), wire feed rate (WFR), and wire tension (WT). The machinability of the composite was evaluated by measuring Surface Roughness (SR), Kerf Width (KW), and Cutting Velocity (CV) during WEDM. Results reveals that the % of Si_3N_4 has greater influence over kerf width and cutting velocity whereas BN % has higher influence over surface roughness. The optimization of process parameters using the Taguchi method resulted in different combinations of parameters for each output response. Therefore, Grey Relational Analysis was applied to determine the common optimal process parameters for all three considered output responses. The identified input parameters that yielded the higher CV, minimal SR and KW were as follows: 0% Si_3N_4 and BN, 6 µs PON, 14 µs POFF, 6 m/min WFR, and 10 g WT. Artificial Neural Network model has been developed to predict the output response CV, SR and KW. The 6–8–3 network model predicts the output responses with better accuracy with overall R^2 value of 99.3% .

Keywords Magnesium composite · Silicon nitride · Wire electrical discharge machining · Taguchi · Grey relational analysis · Artificial neural network

1 Introduction

Metal Matrix Composites (MMCs) are composite materials consisting of two or more materials that possess enhanced properties to meet the specific demands of industries requiring lightweight, high-strength, and wear-resistant materials [1]. These composites are utilized in various engineering sectors such as automotive, aerospace, defence, etc. By incorporating hard ceramic materials into the matrix metal, the strength of the composite is improved, while the addition of solid lubricants enhances its tribological properties [2]. Among the various MMCs, magnesium-based composites have garnered significant attention attributable to their high strength-to-weight ratio. Commonly used reinforcement materials for magnesium MMCs include SiC, Al_2O_3, B4C, MoS_2, Si_3N_4, graphite, TiC, and even fly ash and rock dust [3]. While these reinforcements enhance the material's properties, they also adversely affect its machinability [4]. Traditional machining techniques struggle to process MMCs due to the presence of hard ceramic materials, which lead to rapid tool wear. Consequently, the development of non-conventional machining processes has emerged as a viable alternative for machining these challenging metal matrix composites. Among these non-conventional methods,

✉ S. Sudhagar
kssudhagar.s@gmail.com

1 Department of Mechanical Engineering, Kalaignarkarunanidhi Institute of Technology, Coimbatore, Tamilnadu, India

2 Department of Mechanical Engineering, Centre for Material Science, Karpagam Academy of Higher Education, Coimbatore, Tamilnadu, India

3 Department of Mechanical Engineering, Kongunadu College of Engineering and Technology, Trichy, Tamilnadu, India

4 Department of Mechanical Engineering, Erode Sengunthar Engineering College, Erode, Tamilnadu, India

Published online: 10 March 2024

WEDM is a commonly employed process for cutting complicated shapes in metals.

In the WEDM process, a sequence of electric sparks are generated between the tool and workpiece to shape the material. Typically, a wire made of copper or brass is used as the tool. During machining, dielectric fluid is made to flow continuously to flush the cutting region and to prevent direct contact between the tool and workpiece [5]. Unlike conventional machining methods that rely on mechanical force, WEDM achieves material removal by utilizing electrical energy. In this process, plasma arc is generated by the electric current between the tool electrode and the work, resulting in expulsion of high thermal energy that melts the work [6]. The supply of electric current is in pulsating approach, which result in intermittent development of plasma arc. While extinguishing an electric spark, the dielectric fluid flow eliminates the melted metal and keeps a consistent distance amongst the tool and work. WEDM is suitable for machining all types of conductive materials and is commonly used in the fabrication of fixtures, tools, and dies [7]. However, despite being more capable and cost-effective than conventional methods for machining MMCs, the WEDM process is more complex and involves numerous factors during machining [8]. Key factors that influence the machining performance of WEDM include the properties of the workpiece material, machine settings, dielectric fluid, and tool material [9]. Even a slight adjustment in the combination of these parameters can impact the final quality of the machined part. The performance of WEDM can be assessed by measuring SR, KW, material removal rate (MRR), CV, tool wear (TW), and other relevant factors.

Kavimani et al. [10] performed research on the WEDM of Magnesium–Graphene composite to analyze the impact of material and machine factors affecting the MRR and SR. The parameters investigated included weight% of reinforcement, SiC doping percentage, PON, POFF, and WFR. The experiments were designed using the Taguchi method, and Grey Relational Analysis (GRA) was employed to optimize multiple responses. The results indicated that MRR increased with higher PON and wire feed rate, while surface roughness increased with longer PON. The GRA approach helped identify optimum process parameters that resulted in maximum MRR and minimum surface roughness. Manikandan et al. [11] developed a predictive model using an ANFIS (Adaptive Neuro-Fuzzy Inference System) model to evaluate the machinability characteristics of LM6/SiC/Dunit composite. GRA consolidate multiple responses or variables into a singular response referred to as the grey relational grade, which was then predicted using ANFIS. The duration of the PON was observed to have a significant impact on both the MRR and RA. Kumar et al. [12] conducted an experimental study to examine the effects of various process parameters on the WEDM of an Al/SiC/Gr/Fe_2O_3 hybrid composite. The investigated process parameters included current, voltage, PON, POFF, WFR, and WT. Taguchi method was employed to optimize the parameters, leading to significant improvements in material removal rate (33.72%) and spark gap (27.28%). Based on the ANOVA results, it was found that the PON time had the most significant influence on SR in the studied process. Following PON, peak current and POFF were identified as the next influential factors affecting surface roughness. Kumar et al. [13] studied the machinability of Al/SiC/B4C hybrid composite in the WEDM process. The effect of current, PON time, WFR, and B4C content on KW and cutting speed was analyzed using response surface methodology (RSM). Vijayabhaskar and Rajmohan [14] aimed to optimize the WEDM process parameters for machining magnesium matrix composites reinforced with nano-SiC particles. RSM was employed, and the results showed that voltage and PON were the major contributing factors to MRR. Increasing the voltage resulted in higher MRR but also increased SR. Sadhasivam and Ramanathan [15] used the TOPSIS (Technique for Order Preference by Similarity to Ideal Solution) method to optimize multiple objectives in WEDM of an aluminum composite. The objectives were to minimize SR and maximize MRR. Optimum PON, voltage, and WFR were determined to be 6 μs, 50 V, and 4 m/min, respectively. Voltage was identified as the significant factor affecting MRR, followed by PON. Pattnaik and Sutar [16] developed a predictive model for WEDM parameters using a combination of Taguchi and Neural Network methods. The suggested optimum values for achieving maximum MRR were a PON of 6 μs, POFF of 7/9 μs, current of 6 Amp, and servo sensitivity of 8 mm/min. The developed predictive model demonstrated good performance with less than 5% when comparing the actual values with the predicted values.

Suresh and Sudhakara [6] carried out a study that focused on investigating machining characteristics of aluminium composite reinforced with nano-SiC particles using the WEDM process. They investigated the impact of process parameters such as gap voltage, POFF, PON, and current on MRR and SR. The findings of the study demonstrated that PON and POFF were the key parameters influencing the machining outcomes. Increasing the SiC particle content in the aluminum matrix led to a reduction in MRR and SR. Ravi Kumar [17] focused on optimizing the WEDM machining parameters for Al/WC composite using a desirability-based multi-objective optimization technique. Based on the ANOVA results, it was determined that the weight% of WC had the most substantial impact on MRR, while peak current was the key factor affecting SR. The optimal parameters for maximizing MRR and minimizing SR were identified as peak current of 116.81 A, PON of 4 s, POFF of 9.99 s, WFR of 14.77 mm/min, and WC content of 2.05%. Dey

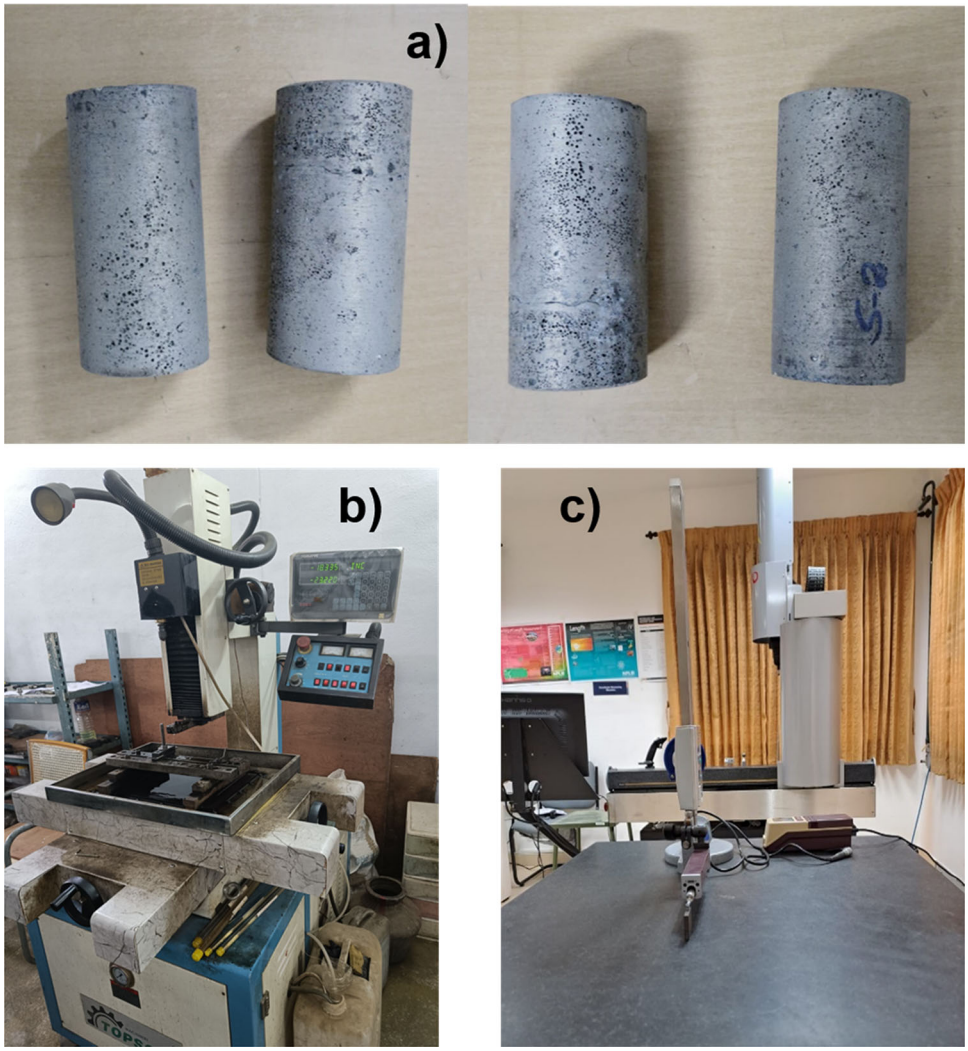

Fig. 1 **a** Fabricated Mg metal matrix composite, **b** WEDM machining setup, **c** Surface roughness measuring setup

and Pandey [18] employed a grey-based multi-objective optimization technique to optimize the PON, POFF, WFR, and weight% of cenosphere during the WEDM of Al/cenosphere composite material. The optimized machining conditions were found to be a PON of 13.992 μs, POFF of 52.00 μs, WFR of 5.398 m/mm, and cenosphere % of 3.209. Gopal et al. [19] utilized GRA to identify a single optimal combination of process parameters for achieving minimum SR and maximum MRR in the WEDM of Mg/CRT/BN composite. Thankachan et al. [20] conducted an optimization study on the WEDM process parameters for friction stir processed Cu/BN surface composite using Taguchi-GRA. Their objective was to achieve maximum MRR and minimum SR. By employing GRA, they identified the optimal combination of input control factors that resulted in the highest MRR (20.19 mm^3/min) and lowest SR (3.01 μs) values.

The manufacturing industries are advancing their technologies towards machining highly complex shapes with high degree of accuracy. Among non traditional machining process, WEDM is most commonly utilized because of minimal material wastage and capability to manufacture complex shapes. Hence, it is the need of the hour to study and improve the machinability characteristic of newly developed composite materials [21, 22]. The literature study showed that most of the WEDM process study were conducted on aluminium MMC and copper MMC. Few studies were dedicated to study the machining characteristics of magnesium matrix composite. In order to bridge this research gap, the current study is intended to investigate the machining characteristics of magnesium metal matrix composite reinforced with Silicon Nitride and Boron Nitride using Taguchi method. Through literature study it has been observed that, different optimum process parameters were obtained for each output response. To overcome the conflict of optimum parameter, a simple multi-objective optimization technique GRA has been utilized to optimise the process parameters. Artificial Neural Network model has been developed to predict the machining characteristic at any combination of process parameters.

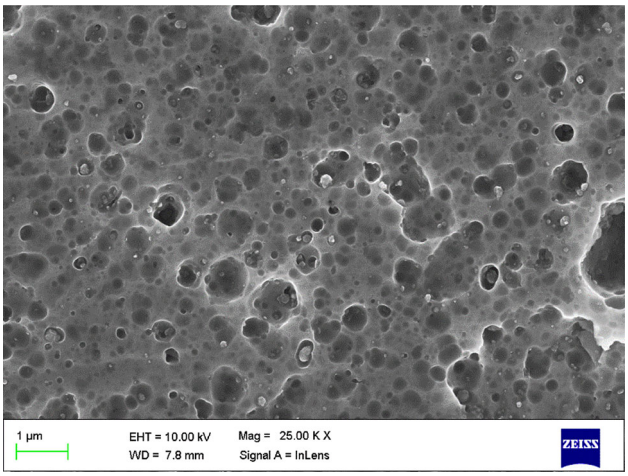

Fig. 2 SEM micrograph of fabricated composite

2 Materials and methods

In this study, the selected matrix material is magnesium alloy, which is widely utilized in aerospace industries. The intention is to enhance the properties of the matrix metal by incorporating different ceramic particles, such as Silicon Nitride (Si_3N_4) and Boron Nitride (BN). Si_3N_4, being a hard ceramic particle, improves the strength and hardness of the matrix metal, while BN, acting as a solid lubricant, enhances its wear resistance. The particle size of the reinforcements used was smaller than 10 µm. To fabricate the hybrid metal matrix composites, the stir casting method, a liquid processing route, was employed. The magnesium matrix metal was melted in a furnace, and a specific amount of the two reinforcement particles was added to the molten magnesium. The mixture was thoroughly stirred using a motor-driven stirrer and then poured into a rectangular die to solidify. Different weight percentages of each reinforcement (0%, 5%, and 10%) were added to examine their effects on the base material's properties. The fabricated composite material is shown in Fig. 1a. The distribution of reinforcement particle in matrix material has been analysed using scanning electron microscopic image shown in Fig. 2. The microscopic image revealed that the reinforced particles were evenly distributed in matrix material.

To investigate the machining characteristics of the developed composites, WEDM controlled by a computer shown in Fig. 1b was utilized. A 0.25 mm diameter copper wire was employed for the machining process, with distilled water as the dielectric fluid flowing at the rate of 9 l/min. The experiments were conducted by varying the input process parameters, including PON, POFF, WFR, and WT. The study involved adjusting each parameter at three different levels, which are specified in Table 1. The range of process parameters was determined based on prior research and preliminary

Table 1 Input process parameters and their levels

Parameters	Unit	Levels		
		I	II	III
Wt% of Si_3N_4	%	0	5	10
Wt% of BN	%	0	5	10
Pulse ON time (PON)	µs	6	10	14
Pulse OFF time (POFF)	µs	14	18	20
Wire feed rate (WFR)	m/min	6	8	10
Wire tension (WT)	g	8	10	12

experiments. L27 orthogonal array was selected for designing experiments in order to reduce number of trials [23, 24] as shown in Table 2. The machining characteristics of the composites were evaluated by measuring three parameters: CS, SR and KW. SR was measured using a Mitutoyo SJ302 model surface roughness tester shown in Fig. 1c, while the kerf width of each experiment was measured using a tool maker microscope.

3 Result and discussion

3.1 Effect of process parameters on kerf width

In the WEDM process, the mechanism of material removal involves the melting and evaporation of metal surrounding the cutting wire, which carries pulsed current. As a result, the width of the cut is slightly larger than the diameter of the cutting wire. Figure 3 demonstrates the impact of considered parameters on the KW produced during WEDM process. As the weight% of Si_3N_4 particles increases, there is an equivalent rise in the kerf width. Likewise, the kerf width initially increases with an increase in the weight% of BN particles, but after reaching 5%, the kerf width gradually decreases. This phenomenon can be attributed to the discharge of sparks amid the electrode wire and the composite, which melts the material and removes the added reinforcement embedded in the base material. The detachment of the reinforced particles along the electrode wire path contributes to the increase in the width of the cut [25]. Kerf width also increases with an increase in PON. This is because a longer PON results in a longer spark duration between the electrodes, leading to a greater heat input. The higher heat input melts more material from the workpiece, resulting in a larger cutting width. The kerf width tends slightly decrease after 10 µs PON, this might be due to excessive increase in PON result in higher electrode wear. The increased electrode wear result in reduction of size of electrode which in turn produces smaller kerf width.

Table 2 Design of Experiments with output responses

Sl. no.	Input parameters						Output reponses		
	Wt % of Si_3N_4	Wt % of BN	PON (μs)	POFF (μs)	WFR m/min	WT (g)	KW (mm)	SR (μm)	CV (mm/min)
1	0	0	6	14	6	8	0.268	1.568	3.374
2	0	0	6	14	8	10	0.272	1.772	3.425
3	0	0	6	14	10	12	0.276	1.928	3.386
4	0	5	10	18	6	8	0.286	1.774	2.769
5	0	5	10	18	8	10	0.289	1.886	2.623
6	0	5	10	18	10	12	0.295	2.120	2.424
7	0	10	14	20	6	8	0.279	1.826	1.957
8	0	10	14	20	8	10	0.282	2.022	2.215
9	0	10	14	20	10	12	0.288	2.480	1.852
10	5	0	10	20	6	10	0.298	1.368	2.350
11	5	0	10	20	8	12	0.301	1.685	2.522
12	5	0	10	20	10	8	0.307	1.642	2.150
13	5	5	14	14	6	10	0.29	2.165	2.700
14	5	5	14	14	8	12	0.294	2.662	2.565
15	5	5	14	14	10	8	0.299	2.988	2.488
16	5	10	6	18	6	10	0.312	2.120	1.757
17	5	10	6	18	8	12	0.315	2.246	1.414
18	5	10	6	18	10	8	0.321	2.332	1.347
19	10	0	14	18	6	12	0.332	1.826	2.407
20	10	0	14	18	8	8	0.336	2.125	1.995
21	10	0	14	18	10	10	0.342	2.420	1.966
22	10	5	6	20	6	12	0.338	1.546	1.333
23	10	5	6	20	8	8	0.342	2.126	1.228
24	10	5	6	20	10	10	0.348	2.120	1.128
25	10	10	10	14	6	12	0.309	2.728	1.863
26	10	10	10	14	8	8	0.314	2.820	1.454
27	10	10	10	14	10	10	0.32	2.698	1.321

The ANOVA for the kerf width was executed to recognize the significant parameters and its influence % on kerf width. Table 3 shows that, except for WT, all the other parameters were found to have a significant impact on the kerf width. The weight% of Si_3N_4 is the major contributing parameter, accounting for 78.4% of the influence on the kerf width, followed by the POFF at 14.9%. The remaining parameters have a lesser effect on the kerf width compared to the weight% of Si_3N_4 and the POFF.

3.2 Effect of process parameters on surface roughness

Figure 4 illustrates the consequence of independent parameters on SR. The composite material becomes more challenging to machine when the amount of ceramic reinforcement in the magnesium matrix increases. The main effect plot clearly demonstrates that an increase in the weight% of both Si_3N_4 and BN leads to higher surface roughness. This effect of higher roughness is concerned to the higher melting temperature of the reinforced ceramic material. During machining, the spark between the electrode and the workpiece easily melts the magnesium matrix material, while the reinforced ceramic material cannot be melted due to its higher melting temperature. As a result, the magnesium matrix material around the ceramic reinforcement in the wire travel path gets melted, causing the reinforcement to protrude out of the machined surface. The increase in the proportion of silicon nitride and boron nitride increases the number of particles in the wire travel path, leading to higher surface roughness due to the existence of more protruding particles on the machined

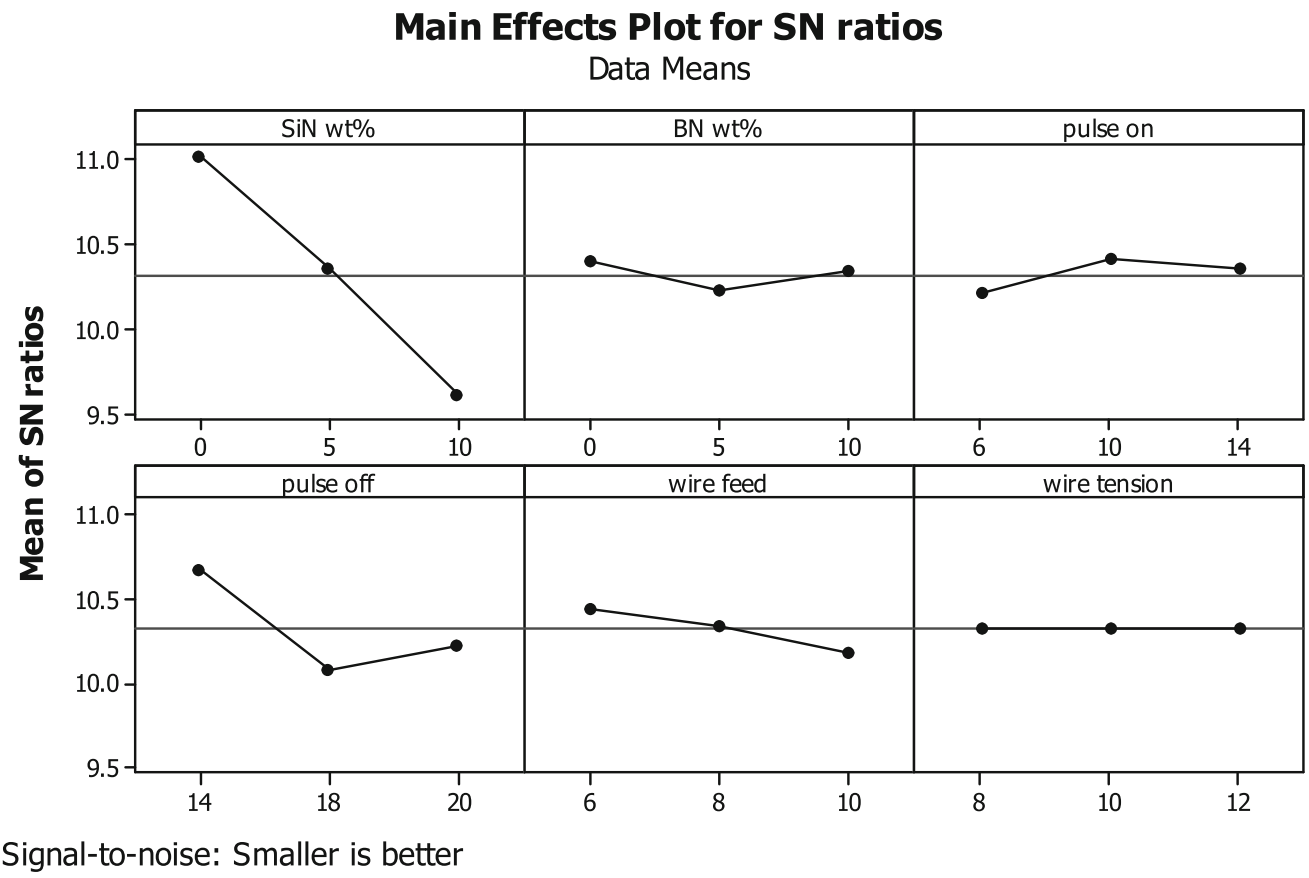

Fig. 3 Effect of process parameter on kerf width

Table 3 ANOVA for kerf width

Source	DF	Seq SS	Adj SS	Adj MS	F	*p*
wt% of Si_3N_4	2	0.011084	0.011084	0.005542	24,938	0
wt% of BN	2	0.000154	0.000154	7.68E−05	345.5	0
PON time	2	0.00031	0.00031	0.000155	696.5	0
POFF time	2	0.002093	0.002093	0.001046	4708.5	0
WFR	2	0.000398	0.000398	0.000199	895.5	0
WT	2	1.6E−06	1.6E−06	8E−07	3.5	0.059
Error	14	3.1E−06	3.1E−06	2E−07		
Total	26	0.014042				

surface [19]. Furthermore, rise in PON results in higher surface roughness during the WEDM process [26]. The PON decides the duration of the electric spark between the electrode and the workpiece. A longer PON cause a longer spark duration, which dissipates more heat and melts more material. The melting of additional material creates craters on the machined surface owing to the presence of reinforcements [27, 28]. These craters contribute to higher surface roughness. Conversely, a higher POFF yields smoother surface during the WEDM process. This can be attributed to the availability of sufficient time to wash away the debris, preventing the recasting of removed material during subsequent sparks. Furthermore, there is a direct relationship between the electrode WFR and the SR value of the machined surface. Specifically, as the electrode WFR increases, the roughness of the machined surface also increases. A higher WFR causes the electrode wire to move faster, introducing a new surface for spark generation. The newer wire surface produces more efficient sparks that penetrate the material deeper, which may be a reason for the higher roughness value.

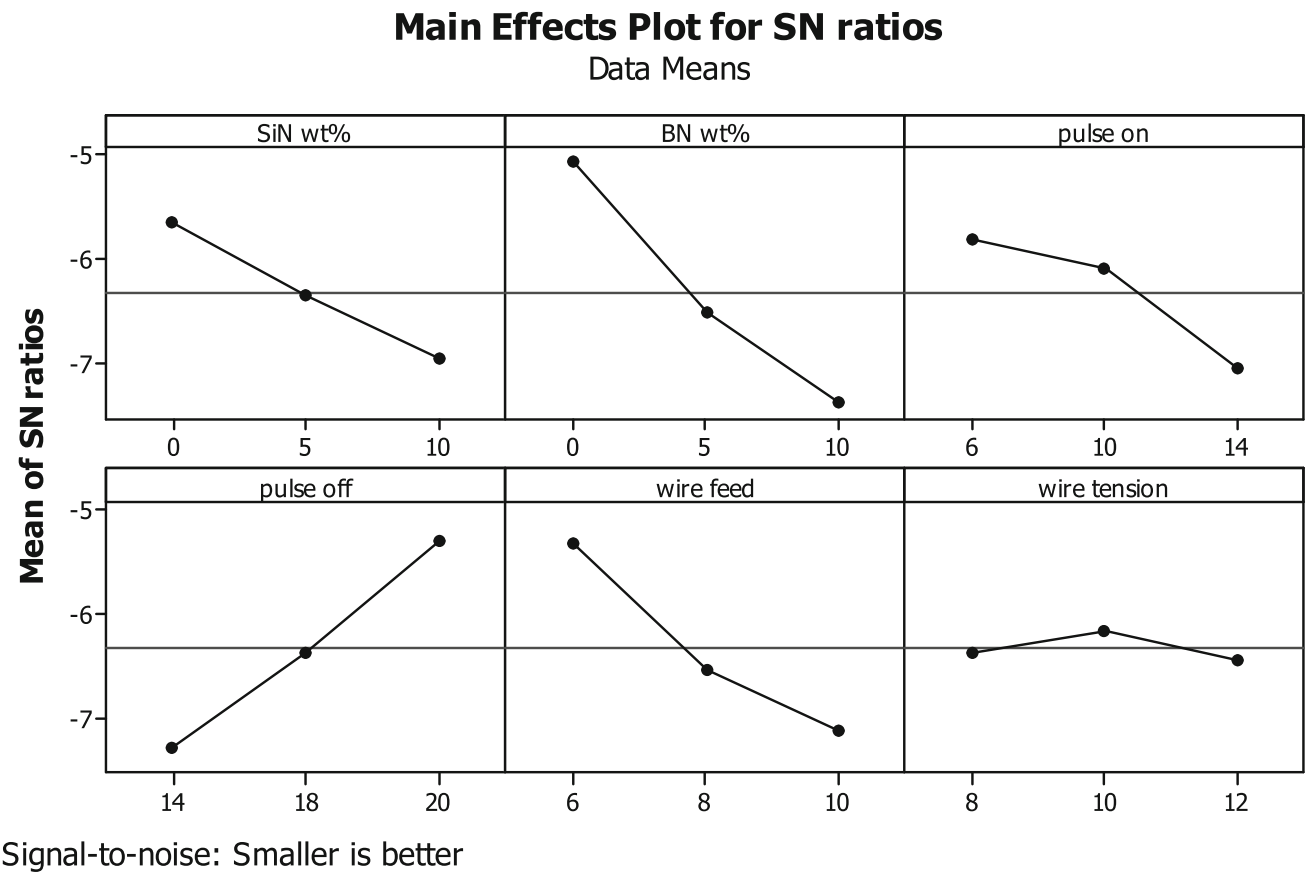

Fig. 4 Effect of process parameter on surface roughness

Table 4 ANOVA for surface roughness

Source	DF	Seq SS	Adj SS	Adj MS	F	*p*
wt% of Si_3N_4	2	0.51843	0.51843	0.25922	11.02	0.001
wt% of BN	2	1.37992	1.37992	0.68996	29.34	0
PON	2	0.43473	0.43473	0.21737	9.24	0.003
POFF	2	1.13569	1.13569	0.56785	24.15	0
WFR	2	0.82517	0.82517	0.41259	17.55	0
WT	2	0.03036	0.03036	0.01518	0.65	0.539
Error	14	0.32918	0.32918	0.02351		
Total	26	4.65349				

ANOVA was performed to ascertain the significance of each process parameter on SR, as publicized in Table 4. The ANOVA was performed at a 95% confidence level, meaning that the parameter having p-value < 0.05 possess significant effect on output response. With the exception of WT, all the process parameters have p-values < 0.05. This implies that WT lacks significant effect on the surface roughness value during the WEDM of Mg/Si_3N_4/BN hybrid composite [29]. Among the significant parameters, the weight% of BN contributes the highest percentage of 29.65% to the SR, followed by the POFF with a contribution of 24.4%. The WFR, weight% of Si_3N_4, and PON contribute 17.73%, 11.14%, and 9.34% respectively to the surface roughness.

3.3 Effect of process parameters on cutting velocity

Figure 5 illustrates the variation of CV regarding change in each process parameter. To optimize the cutting velocity, the "larger the better" option was chosen for the analysis of the

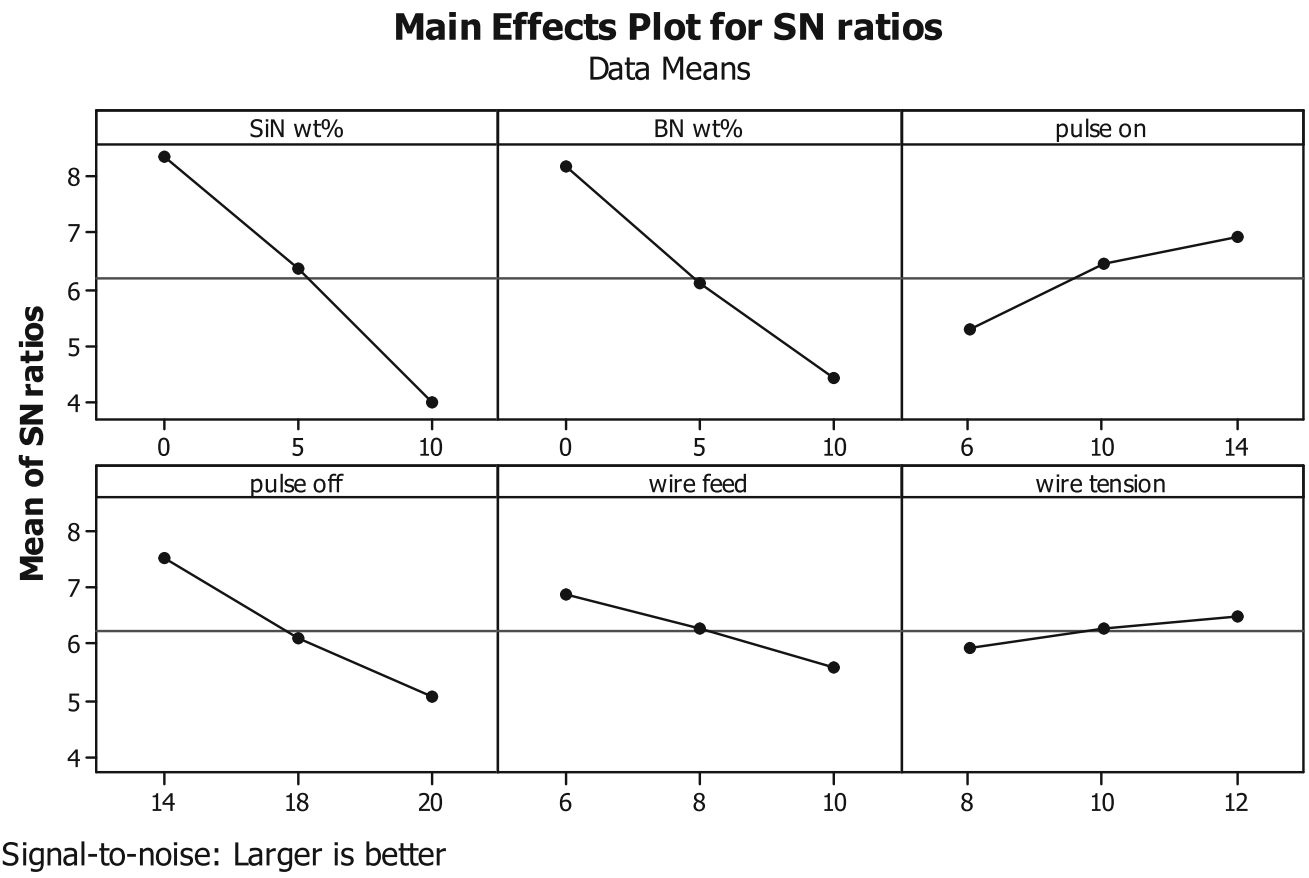

Fig. 5 Effect of process parameter on cutting velocity

Table 5 ANOVA for cutting velocity

Source	DF	Seq SS	Adj SS	Adj MS	F	*p*
wt% of Si_3N_4	2	4.83638	4.83638	2.41819	148.32	0
wt% of BN	2	3.91639	3.91639	1.9582	120.11	0
PON	2	0.17391	0.17391	0.08696	5.33	0.019
POFF	2	1.96275	1.96275	0.98137	60.19	0
WFR	2	0.33471	0.33471	0.16735	10.26	0.002
WT	2	0.05962	0.05962	0.02981	1.83	0.197
Error	14	0.22825	0.22825	0.0163		
Total	26	11.51201				

SN ratio. It is observed that an increase in the percentage of reinforcement particles significantly decreases the cutting velocity. The presence of non-conductive ceramic materials in the path of the electrode wire obstructs spark generation, thereby impeding the forward movement of the wire and leading to a decrease in cutting velocity. Furthermore, an increase in the PON induce increase in cutting velocity. A longer spark duration melts more material around the electrode wire and creates more space ahead of the wire, enabling it to move forward rapidly without any hindrance [30]. Conversely, the POFF, which is the duration without spark, have opposite effect on cutting velocity. An increase in POFF leads to decreased cutting velocity as it extends the idle time without spark, resulting in a slower cutting process [31]. The WFR demonstrates a direct proportionality with cutting velocity. It is known that a higher WFR increases the intensity of the spark, leading to a greater amount of material erosion. Consequently, at higher material removal rates, the cutting velocity tends to be higher as well.

Table 6 Optimum process parameter obtained through Taguchi method

Parameter	Optimum parameter for		
	min Kerf width	min Surface roughness	Max cutting velocity
Wt% of Si_3N_4	0	0	0
Wt% of BN	0	0	0
PON	10	6	14
POFF	14	20	14
WFR	6	6	6
WT	10	10	12
Kerf width (mm)	0.258	0.318	0.293
Surface roughness (μm)	2.166	1.271	2.365
Cutting velocity (mm/min)	2.492	1.985	3.510

Table 7 Grey relational analysis result

Normalization			Grey relational coefficient			Grey relational grade
Cutting velocity	Surface roughness	Kerf width	Cutting velocity	Surface roughness	Kerf width	
0.978	0.877	1.000	0.957	0.802	1.000	0.920
1.000	0.751	0.950	1.000	0.667	0.909	0.859
0.983	0.654	0.900	0.967	0.591	0.833	0.797
0.714	0.749	0.775	0.636	0.666	0.690	0.664
0.651	0.680	0.738	0.589	0.610	0.656	0.618
0.564	0.536	0.663	0.534	0.519	0.597	0.550
0.361	0.717	0.863	0.439	0.639	0.784	0.621
0.473	0.596	0.825	0.487	0.553	0.741	0.594
0.315	0.314	0.750	0.422	0.421	0.667	0.503
0.532	1.000	0.625	0.517	1.000	0.571	0.696
0.607	0.804	0.588	0.560	0.719	0.548	0.609
0.445	0.831	0.513	0.474	0.747	0.506	0.576
0.684	0.508	0.725	0.613	0.504	0.645	0.587
0.626	0.201	0.675	0.572	0.385	0.606	0.521
0.592	0.000	0.613	0.551	0.333	0.563	0.482
0.274	0.536	0.450	0.408	0.519	0.476	0.468
0.125	0.458	0.413	0.364	0.480	0.460	0.434
0.095	0.405	0.338	0.356	0.457	0.430	0.414
0.557	0.717	0.200	0.530	0.639	0.385	0.518
0.377	0.533	0.150	0.445	0.517	0.370	0.444
0.365	0.351	0.075	0.440	0.435	0.351	0.409
0.089	0.890	0.125	0.354	0.820	0.364	0.513
0.044	0.532	0.075	0.343	0.517	0.351	0.404
0.000	0.536	0.000	0.333	0.519	0.333	0.395
0.320	0.160	0.488	0.424	0.373	0.494	0.430
0.142	0.104	0.425	0.368	0.358	0.465	0.397
0.084	0.179	0.350	0.353	0.379	0.435	0.389

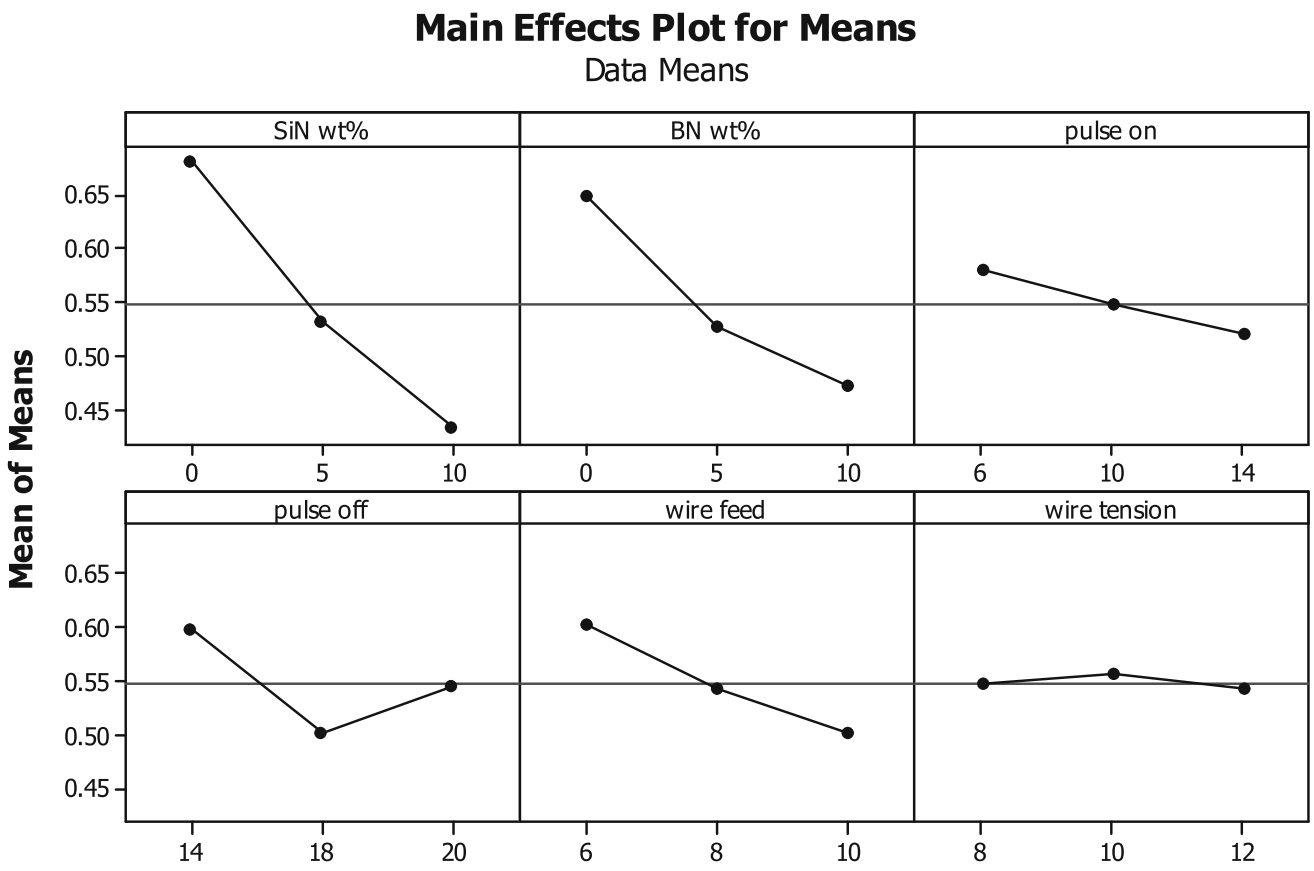

Fig. 6 Effect of process parameters on grey relational grade

ANOVA table for cutting velocity, as shown in Table 5, helps identify the most dominant parameter. Similar to surface roughness, WT does not have a major impact on cutting velocity. However, it was detected that all the other parameters had a noteworthy influence on the output. Among the parameters, the weight% of Si_3N_4 and BN demonstrates the greatest influence on cutting velocity, contributing 42% and 34% respectively. This indicates that the composition of the ceramic particles in the composite material plays a crucial role in determining the cutting velocity. The POFF also has a notable contribution of 17%, while the remaining parameters have relatively minor effects on cutting velocity.

3.4 Single objective optimization of process parameters

The selection of the best process parameters to accomplish minimal KW, minimal SR, and maximum CV was analyzed using Taguchi S/N ratio and summarized in Table 6. Confirmation experiment was conducted by setting the optimum parameter obtained through Taguchi method and the result is shown in Table 6. It is important to note that the optimal parameters for each response are not identical. This means that the parameters that yield the minimum KW may not produce the best surface finish, and the parameters that result in better surface finish may not be optimal for cutting velocity. Consequently, a single combination of process parameters that simultaneously optimize all responses cannot be identified through single-objective optimization. In such cases, multiple-objective optimization techniques can be employed to identify a single optimum combination of process parameters that can achieve better results for all the desired responses [32]. Due to simplicity and ease of calculation, GRA method has been adopted for optimizing the multiple objectives in the current research work. GRA method optimizes all the objectives simultaneously and generate a single optimum result.

3.5 Grey relational analysis

Grey relational analysis (GRA) is part of grey system theory, which is suitable for solving problems with complicated interrelationships between multiple factors and variables. GRA method perform better for the problems dealing with limited, and uncertain data set. GRA method is more suitable for real world problem where data might not be perfectly clear or may contain noise. GRA is multiple objective optimization technique which combines all the objective functions and

transforms the multiple objective problem into single objective problem. The procedure for GRA explained by Sudhagar et al. [33] has been adopted for calculating the normalized value, grey relation coefficient and grey relational grade.

The results obtained from Grey Relational Analysis are presented in Table 7. Among all the experimental trials conducted, trial number 1 achieved the highest grey relational grade of 0.92. This indicates that experimental trial 1 yielded better surface roughness, kerf width, and cutting velocity compared to the other 26 experimental trials. However, it should be noted that only a comparison among the conducted experimental trials can be made based on the table. To identify the process parameters combination that can yield maximum GRG, the mean GRG for each level of the input process parameters needs to be computed. The mean GRG at each level of the input process parameters are shown in Fig. 6. The level with the maximum mean GRG for each

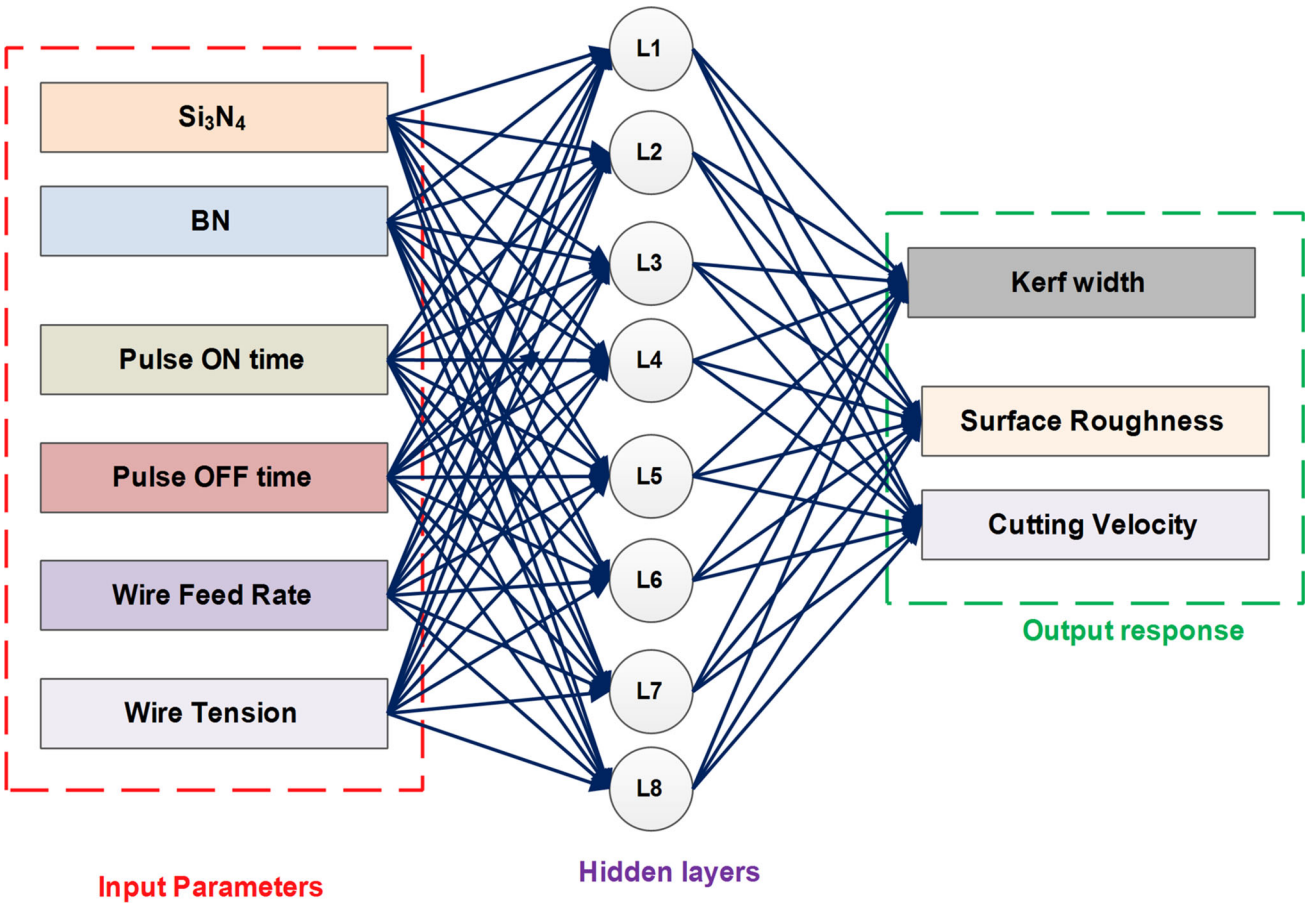

Fig. 7 Neural Network architecture

Table 8 ANOVA for GRG

Source	DF	Seq SS	Adj SS	Adj MS	F	*p*
Wt% of Si_3N_4	2	0.279363	0.279363	0.139681	356.38	0
Wt% of BN	2	0.145078	0.145078	0.072539	185.07	0
PON	2	0.015255	0.015255	0.007627	19.46	0
POFF	2	0.041569	0.041569	0.020784	53.03	0
WFR	2	0.0456	0.0456	0.0228	58.17	0
WT	2	0.001107	0.001107	0.000553	1.41	0.276
Error	14	0.005487	0.005487	0.000392		
Total	26	0.533459				

Table 9 Optimum process parameter obtained through GRA

Wt % of Si_3N_4	Wt % of BN	PON Time (μs)	P OFF time (μs)	Wire Feed in m/min	Wire Tension (g)	Kerf Width in mm	Surface Roughness (μm)	Cutting Velocity mm/min
0	0	6	14	6	10	0.27	1.612	3.398

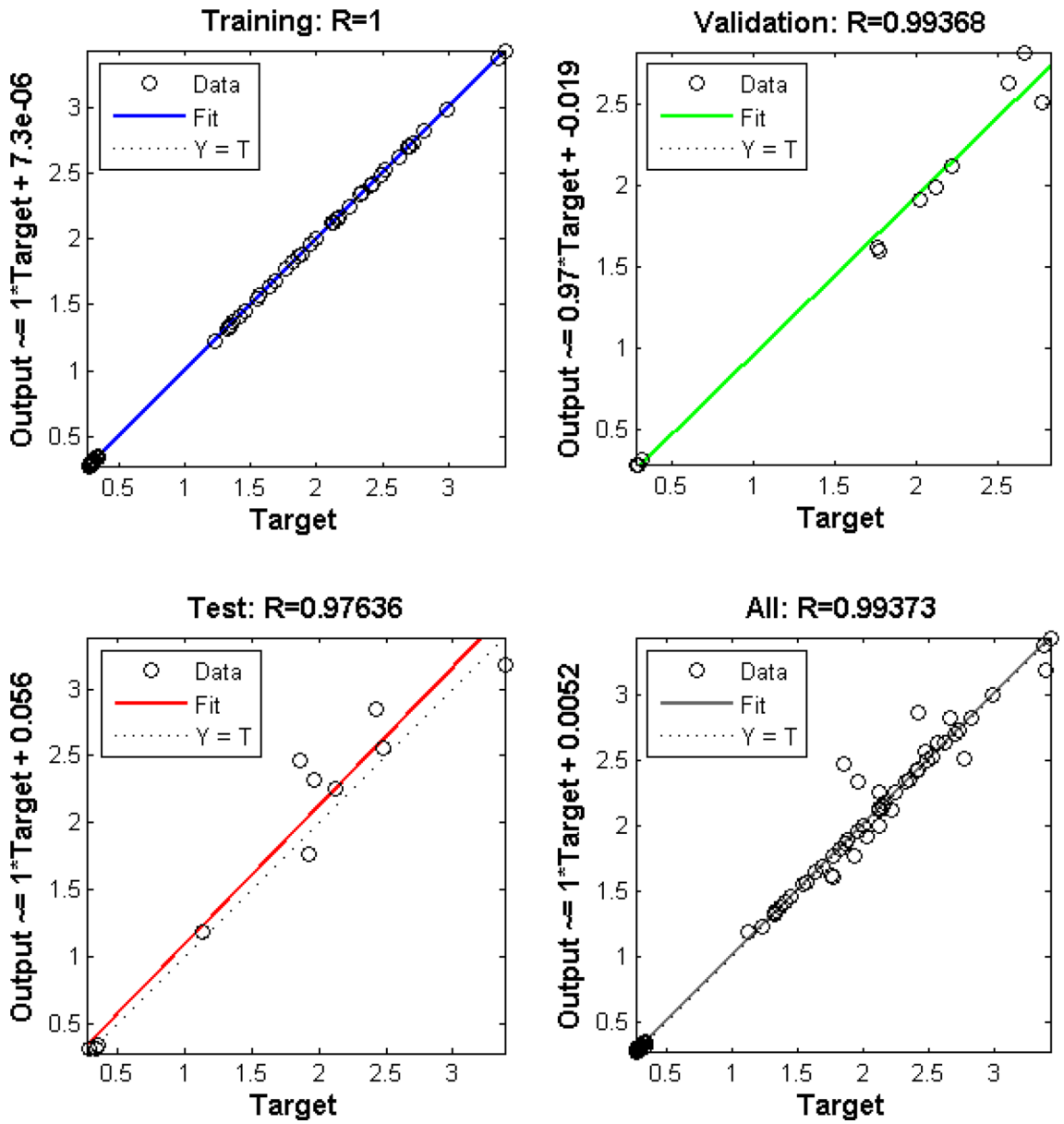

Fig. 8 Regression plot of developed model

process parameter is considered the optimum value. The optimal process parameter combination identified as follows: 0% Si_3N_4 and BN reinforcement percentage, 6 μs PON, 14 μs POFF, 6 m/min WFR, and 10 g Wt. The ANOVA for the GRG was also calculated and presented in Table 8. The process parameters with a *p*-value less than 0.05 are deemed to have a substantial effect on the GRG. According to the ANOVA results, all the process parameters, except for WT, have a significant contribution to the GRG. Confirmation experiment

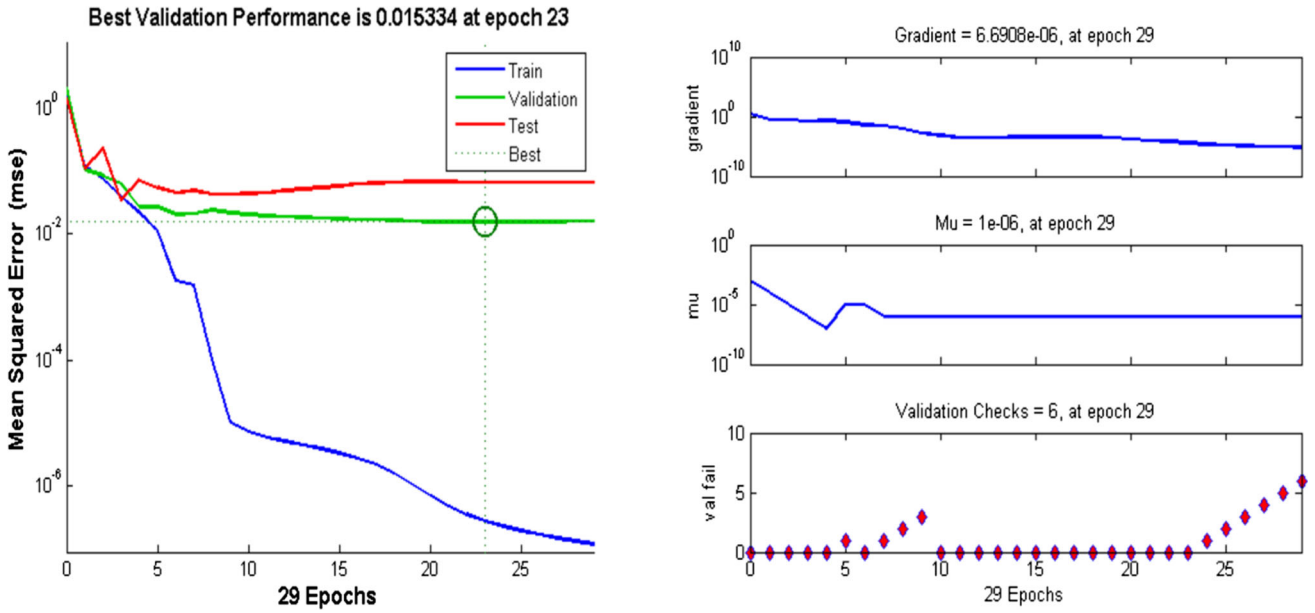

Fig. 9 Performance plot of developed model

was conducted with the GRA identified optimal parameter setting and the result obtained were tabulated in Table 9.

3.6 Neural networks modelling

GRA method have the capability to find the best solution among the given alternatives but it fails to predict the output response for any given input parameter combination. In order to address the shortcoming of GRA method, ANN has been adopted to develop a predictive model. The ANN model has the capability to predict the output response for any given combination of input process parameters with better accuracy. Artificial Neural Networks (ANNs) are of paramount importance when it comes to predicting output parameters in diverse fields, owing to their exceptional capabilities in handling complex data relationships [34]. ANNs have made a significant impact across a wide array of industries and applications. ANNs is inspired by the structure and function of the human brain [35, 36].

In the current work, 70% of the experimental data were used for training ANN and 30% data were used for testing the network model. Among the 27 input values, 19 samples were selected for training the ANN model and the remaining 8 data sets were used for validating the developed model. In this research 6–8–3 architecture (Fig. 7) is used, an input layer with 6 neurons, a single hidden layer with 8 neurons, and an output layer with 3 neurons. Each of these layers serves a distinct purpose in the network's operation. The input layer is responsible for receiving the raw input data or features. In this case, it has 6 neurons, which means that the network expects input data with 6 distinct features or attributes. There is a single hidden layer with 8 neurons. Each neuron in the hidden layer receives input from all 6 neurons in the input layer and performs weighted computations, followed by the application of an activation function. During the training phase ANNs adjust the weights of their connections iteratively using algorithms, to minimize the difference between their predictions and the true target values in the training dataset. The output layer is responsible for producing the network's predictions. In this case, it consists of 3 neurons, indicating that the network is designed to produce 3 distinct predictions. The output layer's neurons receive input from the 8 neurons in the hidden layer and, perform weighted computations and apply an activation function to produce the final output values.

The regression model of trained, tested and validated data sets depicted in Fig. 8. The R-squared (R^2) values indicate the proportion of variance explained by developed model for different datasets. R^2 value of 1 for the training dataset suggests that ANNs model perfectly fits the training data. In other words, model can explain all the variability in the training data, which can be an indication of potential overfitting. R^2 value of 0.99368 for the validation dataset indicates that developed model explains approximately 99.37% of the variability in the validation data. This is a high R^2 value and suggests that model is performing very well on data it hasn't seen during training. It indicates good generalization. R^2 value of 0.97636 for the testing dataset implies that model explains about 97.64% of the variability in the testing data. This is also a strong performance, although it's slightly lower than the R^2 for the validation dataset. It's still indicative of a good model. The overall R^2 value of 0.99373 represents the

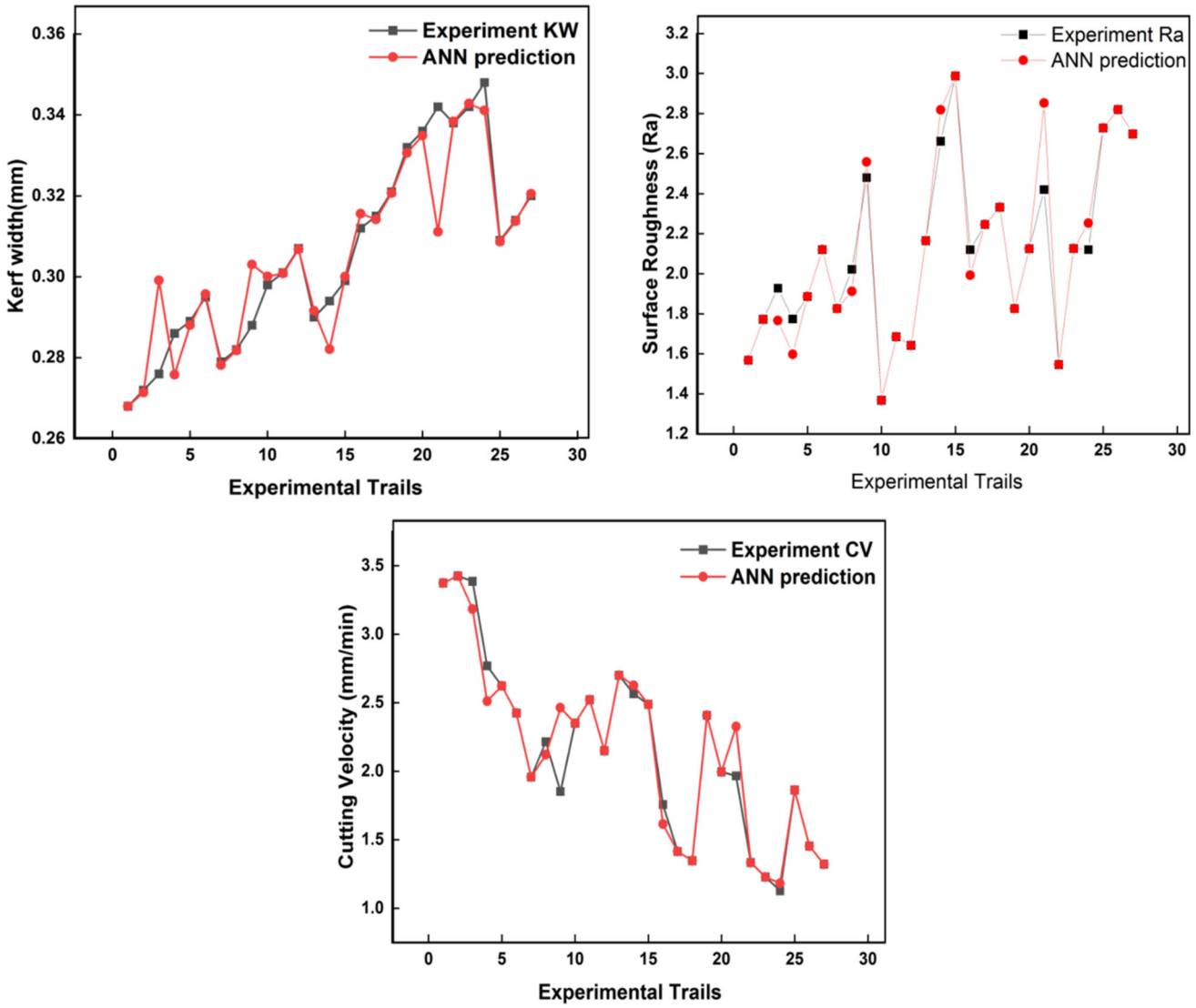

Fig. 10 Experimental VS predicted

Table 10 Comparison between experimental and ANN predicted values

S.l no.	Experimental value			ANN predicted value			% Error		
	KW (mm)	SR (μm)	CV (mm/min)	KW (mm)	SR (μm)	CV (mm/min)	KW (mm)	SR (μm)	CV (mm/min)
1	0.268	1.568	3.374	0.259	1.565	3.316	3.36	0.19	1.72
5	0.289	1.886	2.623	0.284	1.814	2.674	1.73	3.82	- 1.94
6	0.295	2.120	2.424	0.298	2.197	2.451	- 1.02	- 3.63	- 1.11
7	0.279	1.826	1.957	0.275	1.849	1.89	1.43	- 1.26	3.42
16	0.312	2.12	1.757	0.318	2.19	1.69	- 1.92	- 3.30	3.81
24	0.348	2.12	1.128	0.339	2.18	1.141	2.59	- 2.83	- 1.15

combined performance of ANNs model across all datasets, including training, validation, and testing. It suggests that, the model can explain approximately 99.37% of the variability in the data across all sets.

The training and evaluation of neural network model is depicted in Fig. 9. The best validation performance is 0.015334, and it occurred at epoch 23. This indicates that at epoch 23 of the model achieved the lowest validation loss or error, which is a positive sign. Lower validation loss typically indicates better model performance. The gradient value of 6.6908×10^{-6} at epoch 19 represents the rate of change of the loss function with respect to the model's parameters during training. A small gradient value suggests that the model is converging well and may be close to optimal parameter values. Validation checks = 6 at epoch 19 refer to the number of times validation was performed during training. It's common to validate the model's performance at regular intervals (epochs) to monitor its progress and potentially implement early stopping if performance does not improve. Overall information suggests that developed ANN model has undergone training, and at epoch 23, it achieved a good level of validation performance with a low loss and small gradient, indicating that it is learning effectively. From Fig. 10 it can be observed that the trained model has better predictability. The ANN predicted values of output response were compared with the experimental values and the percentage of error was calculated and shown in Table 10. The percentage of error in prediction is less than 5%, this showed that the ANN model predicts the output with better accuracy.

4 Conclusion

Based on the current study and analysis conducted on the WEDM machining of Mg/Si_3N_4/BN hybrid metal matrix composite, the following conclusions can be drawn:

- The addition of ceramic reinforcements Si_3N_4 and BN in the magnesium matrix has a significant impact on the machinability of the material in WEDM. The presence of reinforcements leads to increased surface roughness, kerf width, and decreased cutting velocity.
- The optimal process parameters for minimizing kerf width are 0% Si_3N_4 and BN reinforcement, 10 µs PON, 14 µs POFF, 6 m/min WFR, and 10 g Wt.
- The optimal process parameters for minimizing surface roughness are 0% Si_3N_4 and BN reinforcement, 6 µs PON, 20 µs POFF, 6 m/min WFR, and 10 g Wt.
- The optimal process parameters for maximizing cutting velocity are 0% Si_3N_4 and BN reinforcement, 14 µs PON, 14 µs POFF, 6 m/min WFR, and 12 g Wt.
- The optimal parameters determined through GRA are 0% Si_3N_4 and BN reinforcement, 6 µs PON, 14 µs POFF, 6 m/min WFR, and 10 g Wt which yields 0.27 mm KW, 1.612 µm SR and 3.398 mm/min CV.
- ANOVA showed that all process parameters, except for WT, have a noteworthy influence on the output responses.
- 6-8-3 network model is developed to predict the output response. The overall R^2 value is 99.3% that implies the ANN has better ability to predict the output values.

These conclusions highlight the impact of ceramic reinforcements on the machinability of the Mg/ Si_3N_4/BN composite in WEDM and provide optimized process parameters to achieve desired outcomes in terms of kerf width, surface roughness, and cutting velocity.

Funding No funding was received for conducting this study.

Data availability All the experimental and analyzed data in this study are reported in this article itself.

Declarations

Conflict of interest No potential conflict of interest was reported by the authors.

Ethics approval and consent to participate Not applicable as none of any human participants or animals are involved in the study.

Consent for publication All the authors have read and gave their consent to submit the manuscript for peer review process in the journal for possible publication.

References

1. Kumar, S., Sakthivel, M., Sudhagar, S., Nivethan, K.: Two body abrasive wear characteristics of Al7068/Si3N4/BN hybrid composite. Mater. Res. Express **6**, 66502 (2019)
2. Daniel, A.A., Murugesan, S., Sukkasamy, S.: Dry sliding wear behaviour of aluminium 5059/SiC/MoS2 hybrid metal matrix composites. Mater. Res. **20**, 1697–1706 (2017)
3. Daniel, S.A.A., PM, G.: Study on tribological behaviour of Al/SiC/MoS2 hybrid metal matrix composites in high temperature environmental condition. Silicon **10**, 2129–2139 (2018)
4. Sudhagar, S., Gopal, P.M.: Investigation on mechanical and tribological characteristics Cu/Si3N4 surface composite developed through friction stir processing. Silicon 1–10 (2021)
5. Yusoff, Y., Zain, A.M., Amrin, A., Sharif, S., Haron, H., Sallehuddin, R.: Orthogonal based ANN and multiGA for optimization on WEDM of Ti–48Al intermetallic alloys. Artif. Intell. Rev. **52**, 671–706 (2019)
6. Suresh, S., Sudhakara, D.: Investigations on machining and wear characteristics of Al 7075/nano-SiC composites with WEDM. J. Bio-and Tribo-Corros **5**, 99 (2019)
7. Nag, A., Srivastava, A.K., Dixit, A.R., Mandal, A., Das, A.K., Tiwari, T.: Surface integrity analysis of wire-EDM on in-situ hybrid composite A359/Al2O3/B4C. Mater. Today Proc. **5**, 24632–24641 (2018)

8. Karthik, S., Prakash, K.S., Gopal, P.M., Jothi, S.: Influence of materials and machining parameters on WEDM of Al/AlCoCrFeNiMo0. 5 MMC. Mater. Manuf. Processes. **34**, 759–768 (2019)
9. Saravanan, S., Senthilkumar, P., Ravichandran, M., Shivasankaran, N.: Wire electrical discharge machining of AA6063-TiC particle reinforced metal matrix composites using Taguchi method. Mater. Res. Express. **5**, 106518 (2018)
10. Kavimani, V., Prakash, K.S., Thankachan, T.: Multi-objective optimization in WEDM process of graphene–SiC-magnesium composite through hybrid techniques. Measurement. **145**, 335–349 (2019)
11. Manikandan, N., Balasubramanian, K., Palanisamy, D., Gopal, P.M., Arulkirubakaran, D., Binoj, J.S.: Machinability analysis and ANFIS modelling on advanced machining of hybrid metal matrix composites for aerospace applications. Mater. Manuf. Processes. **34**, 1866–1881 (2019)
12. Kumar, A., Grover, N., Manna, A., Chohan, J.S., Kumar, R., Singh, S., Prakash, C., Pruncu, C.I.: Investigating the influence of WEDM process parameters in machining of hybrid aluminum composites. Adv. Compos. Lett. **29**, 2633366X20963137 (2020)
13. Kumar, S.S., Erdemir, F., Varol, T., Kumaran, S.T., Uthayakumar, M., Canakci, A.: Investigation of WEDM process parameters of Al–SiC–B4C composites using response surface methodology. Int. J. Lightweight Mater. Manuf. **3**, 127–135 (2020)
14. Vijayabhaskar, S., Rajmohan, T.: Experimental investigation and optimization of machining parameters in WEDM of nano-SiC particles reinforced magnesium matrix composites. Silicon. **11**, 1701–1716 (2019)
15. Sadhasivam, R.M.S., Ramanathan, K.: Investigating the parametric effects and analysis of stir cast aluminium matrix composite by wirecut-EDM using topsis method. Sādhanā **46**, 143 (2021)
16. Pattnaik, S., Sutar, M.K.: Advanced Taguchi-neural network prediction model for wire electrical discharge machining process. Process. Integr. Optim. Sustain. **5**, 159–172 (2021)
17. Ravi Kumar, K.: Desirability-based multi-objective optimization and analysis of WEDM characteristics of aluminium (6082)/tungsten carbide composites. Arab. J. Sci. Eng. **44**, 893–909 (2019)
18. Dey, A., Pandey, K.M.: Selection of optimal processing condition during WEDM of compocasted AA6061/cenosphere AMCs based on grey-based hybrid approach. Mater. Manuf. Processes. **33**, 1549–1558 (2018)
19. Gopal, P.M., Prakash, K.S., Jayaraj, S.: WEDM of Mg/CRT/BN composites: Effect of materials and machining parameters. Mater. Manuf. Processes. **33**, 77–84 (2018)
20. Thankachan, T., Prakash, S., Loganathan, K.: WEDM process parameter optimization of FSPed copper-BN composites. Mater. Manuf. Processes. **33**, 350–358 (2018)
21. Manikyam, S., Kumar, P.J.: Experimental investigation and surface quality parameters optimization in WEDM machining of D-series tool steels. Adv. Mater. Process. Technol. **8**, 814–825 (2022)
22. Das, A.D., Kumar, K.S., Prasanna, R.: Investigating the effect of wire cut EDM of titanium alloy 6242 using TOPSIS. Adv. Mater. Process. Technol. **8**, 1–13 (2022)
23. Suresh, S., Venkatesan, K., Rajesh, S.: Optimization of process parameters for friction stir spot welding of AA6061/Al2O3 by Taguchi method. In: AIP conference proceedings. AIP Publishing (2019)
24. Suresh, S., Venkatesan, K., Natarajan, E., Rajesh, S.: Performance analysis of nano silicon carbide reinforced swept friction stir spot weld joint in AA6061-T6 alloy. Silicon. **13**, 3399–3412 (2021)
25. Kumar, S.D., Ravichandran, M.: Synthesis, characterization and wire electric erosion behaviour of AA7178-10 wt.% ZrB2 composite. Silicon. **10**, 2653–2662 (2018)
26. Chen, Z., Zhang, Y., Zhang, G., Li, W.: Investigation on a novel surface microstructure wire electrode for improving machining efficiency and surface quality in WEDM. Int. J. Adv. Manuf. Technol. **102**, 2409–2421 (2019)
27. Ishfaq, K., Anwar, S., Ali, M.A., Raza, M.H., Farooq, M.U., Ahmad, S., Pruncu, C.I., Saleh, M., Salah, B.: Optimization of WEDM for precise machining of novel developed Al6061-7.5% SiC squeeze-casted composite. Int. J. Adv. Manuf. Technol. **111**, 2031–2049 (2020)
28. Maher, I., Sarhan, A.A.D., Barzani, M.M., Hamdi, M.: Increasing the productivity of the wire-cut electrical discharge machine associated with sustainable production. J. Clean. Prod. **108**, 247–255 (2015)
29. Nouri, H.: MBFA algorithm based optimization of tungsten carbide alloy wire cut machining process. Int. J. Interact. Des. Manuf. (IJIDeM). **17**, 307–329 (2023)
30. Mostafapor, A., Vahedi, H.: Wire electrical discharge machining of AZ91 magnesium alloy; investigation of effect of process input parameters on performance characteristics. Eng. Res. Express. **1**, 015005 (2019)
31. Saleem, M.Q., Naqvi, M., Khan, S.A., Mufti, N.A., Ishfaq, K.: Performance evaluation of SiC powder mixed electrical discharge machining: A case of wire cut mode with re-circulating molybdenum wire. Int. J. Adv. Manuf. Technol. **116**, 2197–2210 (2021)
32. Modrak, V., Pandian, R.S., Kumar, S.S.: Parametric study of wire-EDM process in Al-Mg-MoS2 composite using NSGA-II and MOPSO algorithms. Processes. **9**, 469 (2021)
33. Sudhagar, S., Sakthivel, M., Mathew, P.J., Daniel, S.A.A.: A multi criteria decision making approach for process improvement in friction stir welding of aluminium alloy. Measurement (Lond). (2017). https://doi.org/10.1016/j.measurement.2017.05.023
34. Thankachan, T., Soorya Prakash, K., Kavimani, V., Silambarasan, S.R.: Machine learning and statistical approach to predict and analyze wear rates in copper surface composites. Met. Mater. Int. **27**, 220–234 (2021)
35. Kavimani, V., Prakash, K.S., Thankachan, T.: Surface characterization and specific wear rate prediction of r-GO/AZ31 composite under dry sliding wear condition. Surf. Interfaces. **6**, 143–153 (2017)
36. Kavimani, V., Prakash, K.S.: Tribological behaviour predictions of r-GO reinforced mg composite using ANN coupled Taguchi approach. J. Phys. Chem. Solids. **110**, 409–419 (2017)